Numerical simulation on the influence of stirrups during electrochemical repair

Jiayuan Hu
E.Energy Technology Co., Ltd.

Xiao-yu He, Jian Shen
Research Center for Water Transport and Marine Engineering Technology, Zhejiang Provincial Institute of Communications Planning, Design & research Co., Ltd., Hangzhou, Zhejiang

Xin Cheng, Jin Xia, Wei-liang Jin
Institute of Structural Engineering, Zhejiang University

ABSTRACT

Stirrup in the concrete structure has noteworthy effect on the electrochemical chloride removal (ECR), which was always ignored in the numerical simulation. Taking the impact of stirrup into consideration has disadvantages on improving the accurate of modeling results. In this paper, a three dimensional (3D) numerical model considering the impact of stirrup on ECR treatment was established, and an experiment was numerically studied to explore the validity of the model. The difference between the residual chloride concentration of simulation and experiment in most region of the concrete structure is within ± 25%. Based on this model, the effect of stirrups on ECR's efficiency were explored. The results of numerical model shows that the stirrup has shielding effect on the chloride migration of the region between the stirrups, while in the region near the stirrup, it has positive on the chloride removal.

Keywords: chloride ion, reinforced concrete, electrochemical chloride removal, ions migration, numerical simulation, 3D model.

1. INTRODUCTION

In the context of sustainability and whole life costing, Reinforced concrete structure's failure has recently gained considerable attention globally [1,2,3] Unfortunately, the durability of the structure is still significantly threaten by chloride penetration and corrosion[4]. In 1998, the direct cost of corrosion in the United States was about 22.6 billion dollars [5]. In 2014, the total cost of corrosion in China was 74.91 billion RMB [6]. To deal with this worldwide issue, a series of rehabilitation method were developed to solve the problem, such as stainless steel with coating [7], concrete coating [8] and high-performance concrete [9]. Additionally, electrochemical repair have been gradually developed and widely adopted in the last several decades for its fewer side effects and high efficiency. Electrochemical repair involves the application of a direct current through an externally applied anode and catholic steel. Owing to the electrochemical reaction in the internal of the concrete structure, it can not only accelerate the re-alkalization of contaminated concrete structure [10] and remediate the surface crack of the concrete structure [11], but also migrates the harmful ions out of the internal region of structure [12] and inhibit corrosion of rebar [13] simultaneously.

Nowadays, with the widely application of electrochemical remediation, a series of experimental and computational researches have been made to explore the influence factors on electrochemical repair. As experimental study is a time-consuming process and empirical method lack of theoretical basis, numerical simulation has been adopted by many scholars [14,15]. These numerical simulation rarely take the influence of stirrup into consideration. However it was experimentally studied that existence of stirrup was non-negligible on efficiency of ECR. Chang [16] reported that stirrup of the internal concrete structure has influence on ECR efficiency, it can limit the chloride migration out of the region between the stirrups.

In this paper, based on mass conservation, the Nernst–Plank equation, and Gaussian theory as well as considering multi-species coupling in the concrete, a numerical model was theoretically established to determine the effect of the stirrup on the ECR treatment. The shielding effect caused by

the presence of the stirrup was investigated experimentally and numerically. Moreover, according to the modeling results, the stirrup has positiove effects on the transport of chloride ions in the local region close to the RC section with the stirrup.

2. MODEL ESTABLISHEMNT

Based on the mass conservation equation, the transport of different ionic species can be expressed as:

$$\frac{\partial C_i}{\partial t} = -\nabla \cdot J_i \quad i = 1, 2, ..., N \tag{1}$$

Where C_i [mol/m³] is the concentration of the ith ionic species in the concrete, t [s] is the time, J_i [mol/(m²•s)] is the flux of the ith ionic species in the concrete, and N is the total number of ionic species in the concrete.

Under the influence of externally applied electrical field, the chloride ion migration in the chloride-contaminated concrete follows the principle of ionic mass transfer. Owing to the establishment of the mass conservation equation is based on the unit volume of the concrete, the mole number of ions passing through the unit area of the concrete per unit time can be defined as ion flux, which can be described by the Nernst–Planck equation:

$$J_i = -D_i \nabla C_i - z_i D_i C_i \left(\frac{F}{RT} \nabla \Phi \right) \tag{2}$$

Where D_i [m²/s] is the diffusion coefficient of the ith ionic species in the concrete, z_i is the charge of the ith particle ($z_{Ca^{2+}} = 2$), is the Faraday constant (9.648 × 10⁴ C/mol), T is the absolute temperature (298 K), and R is the ideal gas constant [8.134 J/(mol.K)]. Based on the substitution of Eq. (2) into Eq. (1), the following equation can be obtained:

$$\frac{\partial C_i}{\partial t} = D_i \nabla^2 C_i + \frac{z_i D_i F}{RT} \nabla (C_i \nabla \Phi) \tag{3}$$

To solve Eq. (3) and obtain the ionic concentration in the concrete, it can be coupled with the electroneutrality condition by assuming that the total net charge of the concrete is zero:

$$\sum_{i=1}^{N} z_i C_i = 0 \tag{4}$$

During the ECR treatment, electrode reactions occur on the surfaces of the cathodic reinforcing steel bars and anodic stainless-steel mesh. The oxygen absorption and hydrogen evolution reactions on the surface of cathodic reinforcing steel bars can be expressed using Eqs. (5) and (6):

$$2H_2O + O_2 + 4e^- = 4OH^- \tag{5}$$

$$2H_2O + 2e^- = 2OH^- + H_2 \tag{6}$$
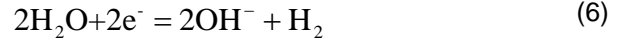
Based on Eqs. (5) and (6), only hydroxyl ions are generated on the surface of the cathodic steel bar, while the flux of all other species is zero. Thus, the flux of the generated hydroxyl ions is equivalent to the externally applied current density:

$$J_{OH^-} = \frac{I}{z_{OH^-} F} \tag{7}$$

The ionic concentration near the anode is assumed to be constant because of the large volume of the anodic electrolyte. The boundary conditions on those where there is no anode or cathode are assumed to have zero flow because of the current density and absence of ionic transport.

3. MODEL VERFICATION AND DISCUSSION

3.1 Experimental details and parameters of the numerical model

In the experiment of scholar Chang et al., the specimen with a dimension of $150 \times 150 \times 300$ mm was prepared. There were four longitudinal steel bars as major reinforcements with the core concrete surrounded by stirrups. The diameter of longitudinal steel bars is 12.3 mm and it is 9.52 mm of the stirrups, as is shown in Fig. 1(a). An amount of chloride for 1.8% cement weight was introduced into the concrete (200 [mol/m³] concrete) for simulating the chloride contaminated concrete. A constant voltage of 20 V was applied for 8 weeks and electrolyte used for anode cell is 100 [mol/m³] NaOH solution. The schematic of the ECR treatment is shown in Fig. 1(b). In the specimen, all longitudinal steel bars and stirrups were connected with the negative pole of the power source acting as cathode, while the stainless steel mesh acting as anode was arranged under the lower surface of the specimen.
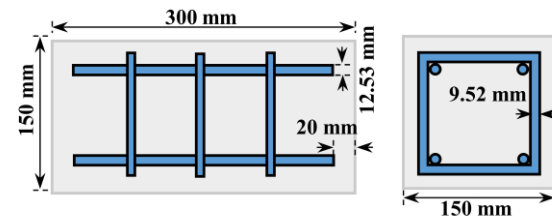
(a) dimension of the specimen

(b) schematic of ECR test

(c) sampling point
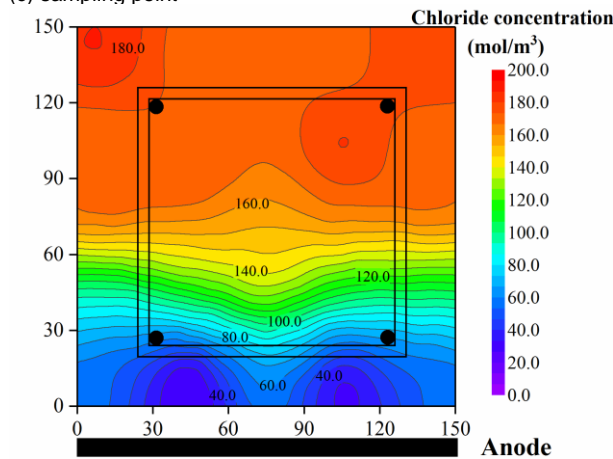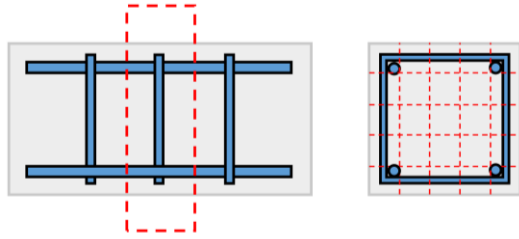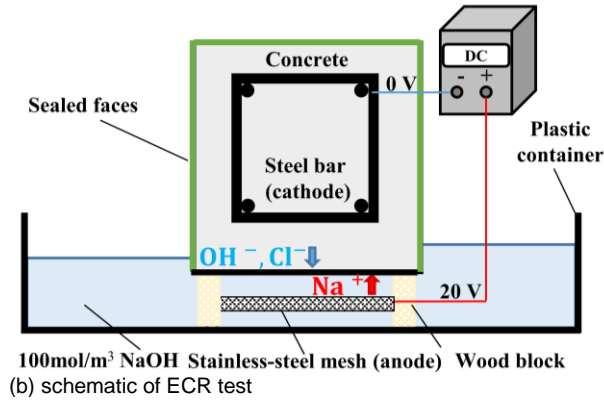
(d) chloride concentration profile
Figure 1. Experimental test of Chang et al.

After the ECR treatment, a slab was obtained from the middle of the RC specimen. The slab was divided into 25 sampling point for chemical titration to determine the water soluble chloride content inside the concrete, as is shown in Fig. 1(c). Then, using these 25 data, the chloride ion concentration contours are generated through the radial basis function approximation. The chloride ion distribution profile obtained after the ECR is shown in Fig. 1(d).

The geometry of the 3D model has the same dimension as that of the experimental specimen (150 × 150 × 300 mm). The initial chloride ion concentration of the concrete, boundary conditions, and diffusion coefficient of different ionic species in the model are listed in Table 1.

Table. 1 Parameters used for numerical model

Ionic species	Boundary concentration (mol/m³)	Initial concentration (mol/m³)	Ion diffusion coefficient D_i (×10⁻¹² m²/s)	Charge number z_i
Cl⁻	10	200	1	-1
OH⁻	50	54.5	2.59	-1
Na⁺	55	200	0.27	1
K⁺	5	50	0.39	1
Ca²⁺	0	2.25	0.16	2

3.2 Chloride distribution

Comparing the chloride concentration obtained by Chang's experiment (see Fig. 1(d)) and numerical modeling (see Fig. 2(a)), the chloride concentration profile is similar. In the region near the side surface of the specimen and region surrounded by the stirrup, the chloride removal rate decreases as the distance from the anodic boundary increases, it confirms the statements of Ihekwaba et.al; in the region near the bottom surface of the specimen, the chloride concentration is significant lower than the other three regions, it mainly owing to that the potential gradient in this region is significant higher than the other regions which is beneficial for the migration of chloride ions. In the region near upper surface of the specimen, the chloride concentration has slight decline and the efficiency of ECR treatment in this region is the lowest compared with the other three regions. Fig. 2(b) shows the difference ratio of the chloride concentration between experiment and modeling ξ [%] varies from -15% to 25% which could meet the tolerance in engineering aspect.

$$\xi = \frac{C_m - C_e}{C_{ini}} \tag{9}$$

where C_m [mol/m³] and C_e [mol/m³] are the chloride concentration obtained by the experiment and modelling respectively; C_{ini} =200 [mol/m³] is the initial chloride concentration of model.
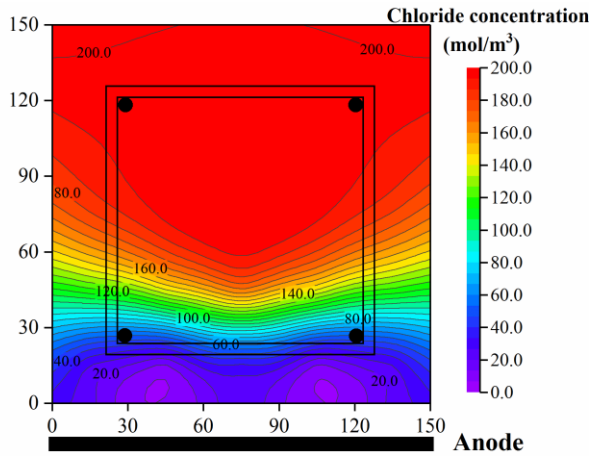
(a) concentration profile of modeling
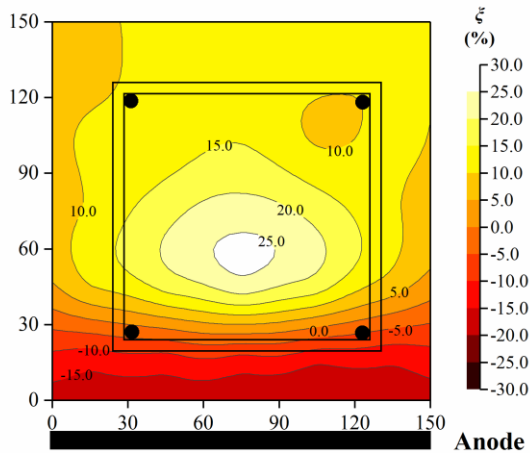
(b) difference ratio of the chloride concentration ξ
Figure 2. Model verification

The chloride concentration of different regions of sections along the length of model is shown in Fig. 3(x=0 and 300 mm corresponds to the side surface of the specimen). In the section with stirrup (x=80mm, 150mm and 220mm), the chloride concentration is lower than the chloride concentration of the adjacent section. In the region between the stirrups (80~150mm and 150~220mm), the chloride concentration increases as the distance from the section with stirrup increases, and the peak value of chloride concentration in this region is higher than the other regions of the model. It might be mainly owing to that the shielding effect caused by existence of stirrups makes the chloride ions in this region is difficult to be removed out. In the section with the stirrups(x=80, 150, 220 mm), the residual chloride concentration is lower than the other sections. It can be explained by that the existence of stirrup induce the potential in this region is lower than the other adjacent sections. The chloride ions can migrate into the adjacent sections under the influence of potential difference.
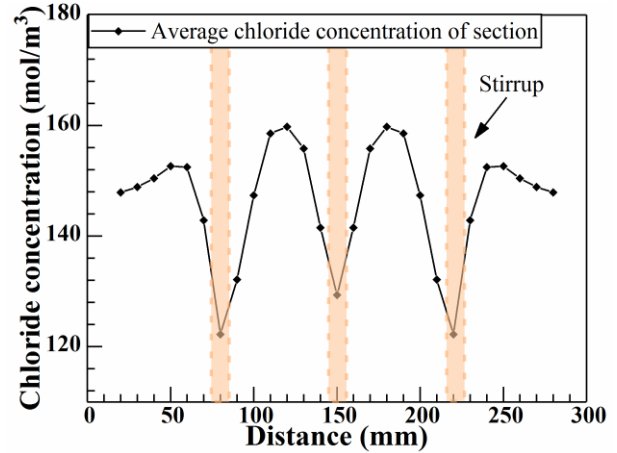
Figure 3. chloride concentration of different sections along the length of model

3.3 Potential distribution

The potential distribution of section with stirrup and section without stirrup is shown in Figs. 4(a) and (b). In the region near side surface of the specimen, compared with section without stirrup, the potential variation in the section with stirrup is more obvious in the region near the anodic boundary and it corresponded to the higher potential gradient which can improve the flux of chloride ions. It leads to that in the region near botton surface of the specimen, the migration rate of chloride ions in the section with stirrup is higher than the migration rate of chloride ions in the section without stirrup. In the region surrounded by the stirrup of section with stirrup, this region enclosed by the stirrup become an equipotential body, the potential is nearly constant 0. While in the corresponding region of section without stirrup, the slightly variation of potential in this region exists. In region near bottom suface of specmen of both sections with stirrup and without stirrup, the potential's variation is more obvious and total flux of chloride ions in this region is higher than the other regions, which causes the chloride removal rate in this part is significant higher than the other regions. Conversely, in region near the upper suface of the specimn, in both section with and without stirrup, the potential is nearly constant 0, and chloride removal rate in this region is nearly 0.

4
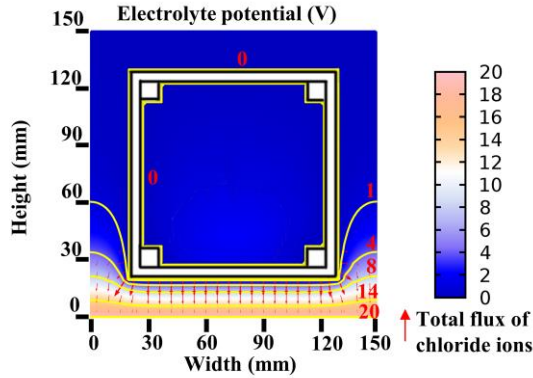
(a) section with stirrup
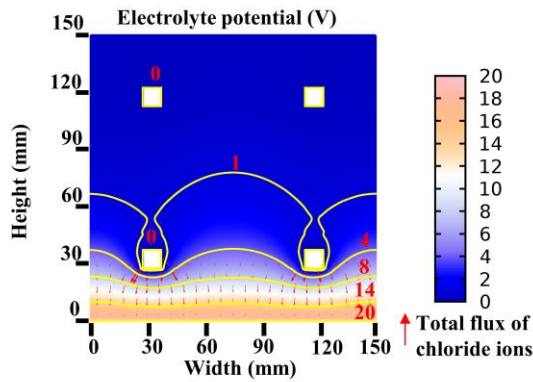
(b) section without stirrup
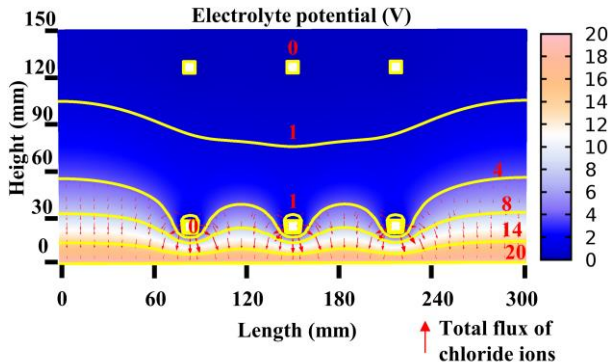
(c) along the length of model

Figure 4. Potential distribution in 3D model

3.4 Influence of stirrup disancte

In Fig. 3, the chloride distribution on the two sides of stirrups is very different. In the region between side surface of model and stirrup (20~80mm and 220~280 mm), as the distance from the section with stirrup increases, the average chloride concentration increases firstly and then descends. It indicates that the influence sphere of stirrup is limited. However, in the region between the stirrups (80~150mm and

150~220mm), the peak value of chloride concentration is in the middle of this region. This might be owing to that the distance between the stirrups is too short, and all the region between the stirrups is still in the influence sphere of stirrup. Thus, considering enlarge the separation distance of stirrup (200 mm) and size of model (150 × 150 × 1000 mm), and keep other parameters of model unchanged. The chloride distribution is shown in Fig. 5.

In the region between the stirrups, the peak value of chloride concentration is not in the central section between stirrups. As the distance from the section with stirrup increases, the chloride concentration increases firstly and then descends. It indicates that in the model with stirrup, the shielding effect makes the chloride ion in the adjacent section of section with stirrup is not easy to be removed. However, the shielding effect influence the local region near the stirrup, as the distance from the stirrup exceed this range, the influence of stirrup would decrease. This can explained that in the region between stirrup and side surface of 3D model (20~80mm and 220~280 mm), although the potential becomes higher as the distance from the side surface decrease (see Figs. 4(c)), the chloride ions has not continually increased. It is because that influence of stirrup becomes less as the distance from the section with stirrup increases, and the phenomenon of ionic transport along the length of model decreases.
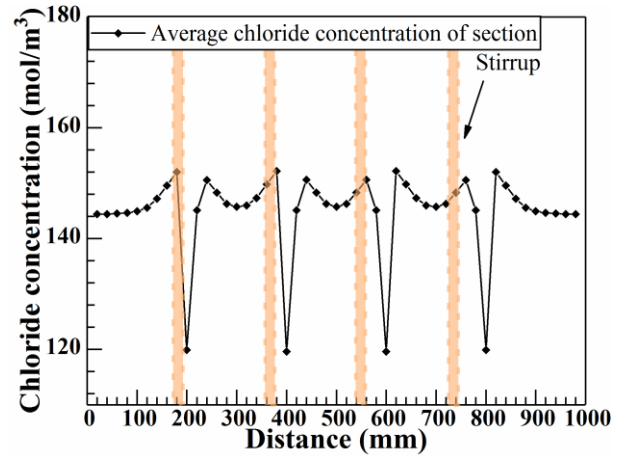
Fig. 5. Chloride distribution along the length of model

Additionally, compared with the modeling results in the Fig. 3, the peak value of chloride concertation in the Fig. 5 is lower, it indicates that the influence of stirrup on the chloride transport will decrease with the stirrup distance increasing.

4. Conclusions

5

1. The stirrup in the RC structure can induce shielding effect and affect the chloride ions transport in the local region near the stirrup of structure during ECR treatment. As the distance from the stirrup increases, the influence of stirrup will decrease.

2. The peak value of chloride concentration is not in the section with stirrup but the adjacent section of section with stirrup. In the section with stirrup, the chloride removal efficiency is the highest which should be paid more attention during ECR treatment.

3. As the distance between the stirrup increases, the influence of stirrup on chloride migration will be less.

4. The model in this study is beneficial for exploring the process of ECR treatment in RC structure. It has advantages on finding the region with lower chloride removal rate of the model where should be paid more attention.

5. ACKNOWLEDGEMENT

REFERENCES

1.Almusallam AA, Khan FM, Dulaijan SU, Al-Amoudi OSB. 2003. Effectiveness of surface coatings in improving concrete durability. Cement and Concrete Composites 25(4):473-481.

2.Chang CC, Yeih W, Chang JJ, Huang R. 2014. Effects of stirrups on electrochemical chloride removal efficiency. Construction and Building Materials 68:692-700.

3.Cheng A, Huang R, Wu JK, Chen CH. 2005. Effect of rebar coating on corrosion resistance and bond strength of reinforced concrete. Construction and Building Materials 19(5):404-412.

4.Elsener B, Angst U. 2007. Mechanism of electrochemical chloride removal. Corrosion Science 49(12):4504-4522.

5.Hou B, Li X, Ma X, Du C, Zhang D, Zheng M, Xu W, Lu D, Ma F. 2017. The cost of corrosion in China. npj Materials Degradation 1(1):4.

6.Ihekwaba NM, Hope BB, Hansson CM. 1996. Structural shape effect on rehabilitation of vertical concrete structures by ECE technique. Cement and Concrete Research 26(1):165-175.

7.Ismail M, Ohtsu M. 2006. Corrosion rate of ordinary and high-performance concrete subjected to chloride attack by AC impedance spectroscopy. Construction and Building Materials 20(7):458-469.

8.Koch GH, Brongers MP, Thompson NG, Virmani YP, Payer JH. 2005. Cost of corrosion in the United States. Handbook of environmental degradation of materials: Elsevier. p 3-24.

9.Li G, Hu F, Wu Y. 2011. Chloride Ion Penetration in Stressed Concrete. Journal of Materials in Civil Engineering 23(8):1145-1153.

10.Li LY, Page CL. 2000. Finite element modelling of chloride removal from concrete by an electrochemical method. Corrosion Science 42(12):2145-2165.

11.Mehta PK, Burrows RW. 2001. Building durable structures in the 21 st century. Indian Concrete Journal 75(7):437-443.

12.Otsuki N, Ryu J. 2001. Use of electrodeposition for repair of concrete with shrinkage cracks. Journal of materials in civil engineering 13(2):136-142.

13.T M. 1991. Durability design and repair of concrete structures: chloride corrosion of reinforcing steel and alkali-aggregate reaction. Magazine of Concrete Research 43(156):155-170.

14.Xia J, Li L. 2013. Numerical simulation of ionic transport in cement paste under the action of externally applied electric field. Construction and Building Materials 39(SI):51-59.

15.Xu C, Jin WL, Wang HL, Wu HT, Huang N, Li ZY, Mao JH. 2016. Organic corrosion inhibitor of triethylenetetramine into chloride contamination concrete by eletro-injection method. Construction and Building Materials 115:602-617.

16.Yeih W, Jiang JC. 2005. A study on the efficiency of electrochemical realkalisation of carbonated concrete. Construction and Building Materials 19(7):516-524.

17.Zhang Y, Jin W. 2011. Distribution of Chloride Accumulation in Marine Tidal Zone along Altitude. Aci Materials Journal 108(5):467-475.